# Nanoscale

Accepted Manuscript


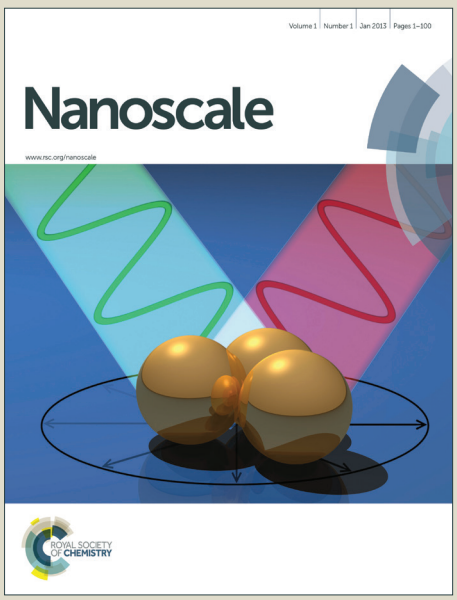





ROYAL SOCIETY OF CHEMISTRY

www.rsc.org/nanoscale

# Time-dependent biodistribution, clearance and biocompatibility of magnetic fibrin nanoparticles: an *in vivo* study

Periyathambi Prabu, Weslen S Vedakumari, Thotapalli P Sastry*.

Bio-Products Laboratory, Central Leather Research Institute (CLRI), Adyar, Chennai 600 020, India.

*Corresponding author.

Tel: +91-9444382361; fax: +91-44-24912150.

Email address: sastrytp@hotmail.com.

**Abstract**

Recently bioretention and toxicity of injected nanoparticles in the body has drawn much attention in biomedical research. In the present study, 5 mg Fe/kg body weight of magnetic fibrin nanoparticles (MFNPs) were injected into mice intravenously and investigated for their blood clearance profile, biodistribution, haematology and pathology studies for a time period of 28 days. Moderate long circulation of MFNPs' in blood was observed with probable degradation and excretion into bloodstream via monatomic iron forms. Inductively coupled plasma optical emission spectrometry (ICP-OES) and Prussian blue staining results showed the increased accumulation of MFNPs in liver, followed by spleen and other organs. Body weight, spleen/thymus indexes, haematology, serum biochemistry and histopathology studies demonstrated that MFNPs were biocompatible. These results suggest the feasibility of using MFNPs for drug delivery and imaging applications.

## 1. Introduction

Currently, nanoparticles (NPs) are employed for diagnosis of diseases in medical field, preservation of food products and cosmetics in industries with different physiochemical properties and many possibilities of human exposure.[1–4] To ascertain biosafety, it is important to consider the potential health impact and mandatory to evaluate time dependent biodistribution, biodegradation and clearance of any nanoparticles introduced into the body. For magnetic iron oxide nanoparticles (IONPs) based system promises to have many biomedical applications such as tumour targeting drug delivery carrier, magnetic resonance imaging (MRI) contrast agents and hyperthermia treatment.[5,6] It is essential to determine the biodistribution, clearance, toxicity and biocompatibility of IONPs depending on their properties such crystalline phase, uniformity size and stoichiometry.[4,7,8] These characteristics can affect cell interaction and serum protein interaction in biological system.

The benefit of using magnetic NPs in clinical field is their ease of *in vivo* detection by magnetic and non-magnetic analysis.[9,10] Non-magnetic analysis of iron element studies such as ICP-OES and Prussian blue staining are observed in the IONPs distribution of tissues.[11] Vibrating Sample Magnetometer (VSM) studies are used to quantify the presence of IONPs in dry tissues by the magnetic analysis.[12] Mostly, the injected IONPs are rapidly cleared by tissue macrophages of the reticuloendothelial system (RES) and the mononuclear phagocytic system (MPS) from blood stream, leads to increased biodistribution in both liver (80-90%) and spleen (5-8%).[13–15] In previous studies, iron oxide nanoparticles were synthesized from goat blood and then functionalized with fibrin to obtain Magnetic fibrin nanoparticles (MFNPs), which is used as a carrier of targeted delivery in clinical studies.[16] Herein, we demonstrated the biodistribution, clearance, toxicity and biocompatibility of MFNPs in mouse model.

## 2. Experimental section

2.1. Materials

Fluorescein isothiocyanate (FITC), sodium phosphate (mono- and di-basic), potassium ferrocyanide, nuclear fast red solution, and 10% neutral-buffered formalin were obtained from Sigma-Aldrich. All the other chemicals used in this study were of analytical grade.

2.2. Preparation of MFNPs

MFNPs was prepared by precipitation methods using goat blood as starting materials to ensure nanoparticle crystalline and superparamagnetic with in vitro biocompatibility according to method reported earlier.[16] The morphology and size of the MFNPs were studied using transmittance electron microscope (TECNAI FE12 TEM instrument operating at 120kV). The hydrodynamic size and surface charge of MFNPs in the PBS solution were evaluated using a dynamic light scattering (DLS) instrument (Malvern Zeta Sizer). Approximately 1 X $10^5$ Saos2 cells were seeded in 6 well. After recovering for 24h, cells were incubated with 50 µg Fe/ml of MFNPs at $37^0$C for 5h. The cells were rinsed with PBS, and stained with Prussian blue for iron to investigate the cellular internalization of MFNPs using microscope.

2.3. Hemolysis assay

The hemolysis assay was carried out to determine whether MFNPs could cause any damage to red blood corpuscles (RBCs) when used for in vivo application.[3] RBCs were collected after removing serum from the blood by centrifugation and suction. RBCs were washed thrice with PBS and used for the assay. The 500 µl of cell suspension were treated with different concentrations of MFNPs - 50, 100, 200, 400, 600, 800, 1000 µg Fe/mL and incubated at room temperature for 120 min. The cell suspensions treated with PBS and deionized water was used as negative and positive control. After incubation, the samples were centrifuges and the absorbances of the supernatants were read at 541 nm.

2.3. Preparation of FITC-labeled MFNPs (FITC@MFNPs)

FITC@MFNPs was prepared by method described elsewhere.[17] Briefly, a solution of FITC (5 mg) in an ethanol/water mixture (1/1, v/v) was added to a dispersion of MFNPs (20 mg) in PBS (20 mL; pH 7.4). The reaction proceeded for 5 h at 20ºC in the dark. The FITC@MFNPs were magnetically separated and washed several times with PBS (pH 7.4) to remove non-conjugated FITC. The fluorescence spectra of FITC@MFNPs were measured by a Jasco FP 6200 spectrofluorimeter (Jasco Analytical Instruments, Easton, MD, USA). The iron levels of FITC labelling and without labelling of MFNPs were measured using the 1, 10-phenanthroline colorimetric method.[10,18]

2.3. *In vivo* study

Balb/c female mice (5–6 week old) weighing around 20–22 g were used for this experiment. All the animals were subjected to humane care, maintained in hygiene conditions and administered with mice pellet feed and water *ad libitum* throughout the experimental period. All experiments were performed after obtaining approval from the Institutional Animal Ethics committee of Central Leather Research Institute, India (466/01a/CPCSEA). The animals were divided into two groups i.e., control and experimental groups. The experimental animals were administrated with 100 μL of MFNPs solution at a dose of 5 mg Fe/kg. The mice were weighted and assessed for their behavior and symptoms every other day for 28 days after post administration.[10, 19, 20]

2.4. Blood clearance experiment

To assess the clearance of FITC@MFNPs *in vivo*, NPs (5 mg Fe/Kg) was injected intravenously to the animals (n = 6) and blood was collected at various time intervals (1h, 3h, 9h, 12h, 24h and 48h). Serum was isolated from the collected blood samples, analyzed using spectrofluorometer at an excitation wavelength of 485 nm and emission wavelength in the range of 500–600 nm.

2.5. Non-magnetic biodistribution methods

2.5.1. Inductively coupled plasma optical emission spectrometry (ICP-OES)

The tissue distribution of MFNPs in mice (n = 6) was studied at the time period of 6h, 12h, 1d, 7d, 14d, and 28d after injection. Immediately after sacrificing the animals, liver, spleen, lungs, heart, and kidney were excised, weighed and lyophilized. Urine and feces were collected and analyzed clearance of injected nanoparticles for 6h, 12h, and 24h, 3d, and 7d. All the samples were heated at 70ºC with nitric acid and 30% $H_2O_2$ at (1:2) concentration until to obtain clear solutions and measured by ICP-OES.[14] All Results were normalized in units of percentage of injected dose per gram (% ID/g) of tissue.

2.5.2. Prussian blue staining

Prussian blue is a highly sensitive method for determination of ferric molecules in tissue sections. To determine MFNPs biodistribution in the major organs such as liver, spleen, lung, kidney and heart, these tissues were fixed in 10% paraformaldehyde and embedded in paraffin. 4 μm thick tissue sections were incubated with fresh 1% potassium ferrocyanide and 1% hydrochloric acid (1:1) for 20 min at room temperature, where this solution stained MFNPs as dark blue/brown and nuclear-fast red was used to stain the nuclei red.[21] All the stained sections were observed under a bright field microscope.

2.6. Magnetic biodistribution method

Biodistribution and clearance of magnetic nanoparticles were measured by the magnetic characterization of tissues in a Lakeshore VSM 7410 at 150 K. According to the ICP-OES studies, most of the IONPs were accumulated in the liver after injection.[5] The liver was excised from the animals (n = 4) at 6h, 12h, 24h time periods and lyophilized. Magnetization curves were recorded by saturating the sample in a 1 T field and sweeping the field range between 1 T and –1 T at 0.1 $Tmin^{-1}$.

2.7. Determination of body weight and immune response

Body weight is an important indicator for evaluating the toxicological effects of the nanoparticles, *in vivo*. After MFNPs injection, the animals were weighed daily and assessed for behavioural changes. To explicitly examining immune response, the spleen and thymus were excised, weighed and the thymus/spleen indices ($S_x$) was expressed accordingly.[22]

Sx = Weight of experimental organ (mg) / Weight of experimental animal (g)

2.8. Haematology and biochemical parameters

Whole blood and serum was collected from the MFNPs injected animals after the time period of 1d, 14d, 28d and series of parameters such as white blood cells (WBC), red blood cells (RBC), platelet count (PLT), haemoglobin (HGB), Haematocrit (HCT), creatinine (CREA), blood urea nitrogen (BUN), aspartate aminotransferase (AST), alanine aminotransferase (ALT) were measured.

2.9. Histopathology

A portion of liver, spleen, heart, lung and kidney tissues excised from the MFNPs injected animals were fixed in 10% neutral buffered formalin and embedded in paraffin. 4 μm thick sections were prepared and stained with Haematoxylin and Eosin (H&E) and viewed under a Nikon Eclipse E600 microscope.

2.10. Statistical analysis

All data presented here as mean ± standard deviation (SD) and analyzed for statistical significance using one-way analysis of variance (ANOVA) followed by Duncan's test. Statistical comparisons in biodistribution studies were determined using the student's *t* test with a significance of $p < 0.05$.

**3. Results and discussion**

Previously, our group has reported the synthesis and characterization of MFNPs along with *in vitro* studies.[16] The study reveals that synthesized MFNPs are crystalline in nature with super-paramagnetic behaviour.[16] Particle size and surface charge properties play an important role

in the in vivo behaviour of synthesised nanoparticles. Under TEM (Fig 1a), MFNPs were spherical in shape with diameter of 12-15 nm. The DLS measured hydrodynamics size distribution and surface charge of the MFNPs were 26.3 nm and – 17.8 mV respectively (Fig.1b and c). The cellular internalization of the MFNPs by Saos2 cells was studied by Prussian blue iron staining method. The microscopic images of stained cells showed a more number of NPs were observed in the cytoplasm and nucleus, there by indicating the increased uptake of MFNPs in treated cells (Fig. 1d). It has been proposed that particles with size less than 100 nm are preferentially taken up by the cells. Also, particles with such miniature size hold larger surface area and result in excessive drug loading capacity with slow rate of drug diffusion. The negative surface charge of MFNP helps repel each particle in suspension, thus confirming their long-term stability and avoidance of particle aggregation.[23, 24]

Hemolysis is a crucial toxicological factor that must be considered for the in vivo practice of MFNPs. As shown in Fig. 1e no sign of visible hemolysis was observed with any of the concentrations of MFNPs used for the analysis. According to ASTM standard F756, the samples exhibiting percentage of hemolysis < 2 are considered as non-hemolytic, 2-5 as slightly hemolytic and > 5 as haemolytic. Our results state the non-hemolytic property of MFNPs and their safety for in vivo application. The hemocompatibility of MFNPs may be ascribed to their negative surface charge. RBCs are made up of two sublayers - a positively charged internal layer and a negatively charged external layer. When positively charged nanomaterials come in contact with the negatively charged RBCs, they instigate the release of toxic substances resulting in hemolysis.[25,26] MFNPs show good internalization potential and hemocompatible, hence can be employed in clinical studies and drug delivery applications. Normally, the distribution of IONPs was difficult to interpret from the results obtained via elemental analysis of Fe in blood samples due to the presence of endogenous Fe like haemoglobin, ferritin and transferrin.[5] In this study, we are using fluorescence marker

labelled with synthesized nanoparticle. Fig.2a illustrates the conjugation of FITC to the MFNPs as determined by fluorescence spectroscopy. It was observed that the peak position of fluorescence emission for the FITC@MFNPs is about 519 nm, a blue line shift of 6 nm as compared to the free FITC in water (525 nm). No fluorescence was observed in the spectrum of the supernatant after washing of the FITC-labelled MFNPs, which is used to track blood circulation in animals. This result confirmed that the MFNPs were successfully modified with FITC via the formation of a stable bond without fluorophore degradation.[17]

With the development of nanocarrier, the blood circulation half time is desired to help the bioavailability of drug. Fig. 2c depicts the blood clearance profile of FITC@MFNPs in experimental animals. Disappearance of MFNPs in blood was increased significantly after 1 h of administration followed by gradual elimination of NPs from blood stream after 3-12 h. MFNPs exhibited a little slowly clearance with the carrier levels of 3.96 % at 24h after administrated nanoparticles. A very less quantity of MFNPs was found in the circulation after 48 h and the blood circulation half-time ($t_{1/2}$) of injected nanoparticles was 12.06 h indicating relatively moderate long circulation and therefore suitable for targeted drug delivery applications. It is supposed that surface charge and particle size of MFNPs have played a vital role in the prolonged blood circulation of NPs by reticuloendothelial cells.[15,27,28]

Biodistribution and tissue-specific accumulation of the NPs have tremendous significance in targeted drug delivery applications. Quantification of iron by ICP-OES was performed at different time periods for major organs including liver, spleen, heart, lung and kidney were shown in Fig. 3a. About 53.11±1.04 ID/g % of the administered NPs were accumulated in the liver, 4.23±1.72 ID/g % in the spleen, 2.81±0.21 ID/g % of iron in the lung, 1.92± 0.37 in kidney and 1.87±0.31 ID/g % in heart at 6 h. The Fe level was continuously depleted after 12 h to 3 d, and then gradually declined over the next 14 d in the liver. While in the case of lung, kidney and heart, the level of Fe decreased after 3 d of injection. But in case of spleen after

12 h the level of injected MFNPs has been increased on 24h and 3d then it has decreased on gradually. The presence of injected MFNPs in spleen at 28 days may be attributed to formation of the monatomic irons and recycling of RBCs, which is in good agreement with the Prussian blue staining results.[10] Based on ICP-OES analysis, most of the administered MFNPs accumulated in the liver which was determined by analyzing the magnetic saturation of the lyophilized samples. The magnetization was 0.064 emu $g^{-1}$ after 6 h of MFNPs administration which gradually declined to a value of 0.03 emu $g^{-1}$ and 0.0036 emu $g^{-1}$ after 12 h and 24 h respectively as shown in Fig. 3b. Hence, we determined the distribution of administered MFNPs, then degradation and clearance of NPs by reticuloendothelial system in liver. Particle size and surface charge of nanoparticles play essential roles in tissue distribution. Iron oxide nanoparticles with size less than 50 nm escape opsonisation and have prolonged circulation time followed by gradual uptake by macrophages in liver and spleen. In the present study, the increased uptake of MFNPs by liver may be ascribed to their smaller size and also net negative surface charge. Earlier studies indicate that the strong negative charges on the surface of nanoparticles enable their uptake by the liver.[30] Tab. 1 shows the clearance of MFNPs in urine and fecal samples at 6, 12, and 24h of post injection. Excretion of nanoparticles in urine and feces studies shows around 7.68 % after 1d and totally 11.67 % after 7 days. Some studies report 18-22% of iron oxide nanoparticles have been slowly cleared over the period of 7 weeks and on the other hand, nearly 25% of iron oxide nanoparticles were more rapidly cleared in 19 days via urine and feces due to the surface chemistry of the magnetic nanoparticles. [29,31]

The tissue sections stained with Prussian blue were examined for iron accumulation, where time-dependent degradation and clearance of the NPs accumulated in liver, spleen and lung kidney and heart were observed (Fig. 4). On 1 d and 7 d MFNPs were found to be predominantly accumulated in the kupffer cells of liver that are located in the linings of the

sinusoids followed by reduced level of staining on days 14 d and 28 d. The injected MFNPs were completely cleared from the kupffer cells by the liver macrophages. The spleen sections showed similar degree of iron staining in all sections due to the rupture of senescent erythrocytes and following release of the iron in the heme group.[10,32–34] A very minimal staining pattern was noticed on 1 d in the lung, kidney and heart sections. Iron nanoparticles are generally excreted from the body via two ways - particles with size less than 5.5 nm are cleared through renal filtration where as larger particles are stored in monatomic form at spleen and blood stream and undergo hepatobiliary (HB) process leading to gradual excretion.[31, 35] In the present study the results obtained using ICP-OES, VSM and Prussian blue staining methods indicat that the injected MFNPs accumulated mostly in the RES organs, then degraded and excreted into the bloodstream in various monatomic iron forms, and then it may gradually clear by HB process.[35-37]

Change in body weight is one of the important criteria to evaluate the NPs toxicity in experimental animals.[38] Fig. 5a depicts measurement of changes in the body weight of control and MFNPs injected experimental animals which were recorded every 2 days up to 28 days. MFNPs at the dose of 5 mg Fe/kg body weight did not cause any mortality in experimental animals compared to the control after 1 d. The body weight of the MFNPs injected experimental animals increased in a fashion similar to that of control animals and there was no significant change between these two groups. After 28 d of MFNPs injection, the experimental animals showed no signs of adverse side effects like dishevelled hair, immobility, convulsions, irregular respiration, gastrointestinal symptoms, severe decubitus paralysis exploratory behaviour as well as neurological disturbance. Necropsy of the animals at the end of the experiment did not show any macroscopic changes of the organs.

As in Fig. 5b, the organ indexes of spleen and thymus were examined on 1 d and 28 d of MFNPs injected experimental animals to grade the changes caused by malities, spleen and

thymus indexes (Sx). As previously reported, a marked rise in the spleen index was noticed in the MFNPs injected experimental animals in this study.[38,] MFNPs injected mice on 1 d, spleen index had no significant change, while the thymus index had very less significant changes due to some kind of protected NPs.[39,] MFNPs injected mice for 28 d showed no significant changes in spleen and thymus indexes compared to control.

Since MFNPs administered intravenously interact primarily with blood and its components, it is necessary to study the level of haematological and serum biochemical indictors after their administration. Fig. 6 illustrated the Haematological and typical biochemical parameters relevant to liver and kidney function, where the levels of white blood cells (WBC), red blood cells (RBC), platelet count (PLT), haemoglobin (HGB), hematocrit (HCT), creatinine (CREA), blood urea nitrogen (BUN), aspartate aminotransferase (AST), alanine aminotransferase (ALT) were unaltered in MFNPs injected experimental animals compared to control. The results suggested no significant toxicity in MFNPs injected animals at the time period of 1, 14 and 28 d and these results are in good agreement with the earlier reports.[40-42]

Evaluation of the tissue morphology was performed to determine the difference between the control and MFNPs injected experimental animals. Fig. 7 shows representative photographs of H & E stained tissue sections of major organs taken during 1, 7, 14 and 28 d of MFNPs injection and compared to the control tissue sections. The liver sections showed normal hepatocyte morphology without inflammatory infiltration. Spleen sections showed no hyperplasia. The lung tissues appeared normal without any sign of pulmonary fibrosis. No hydropic degeneration was observed in heart sections. In the kidney sections, the renal cortex and the glomerulus structure appeared normal and it can be distinguished easily. Overall, the histological analysis showed no necrosis or lesions in any of the major organs in the MFNPs injected experimental animals until 28 days.

## 4. Conclusion

In this study, the time dependent *in vivo* distribution and biocompatibility profile of MFNPs were studied for a period of up to 28 days. The nanoparticles injected in mice were found to be accumulated at a higher percentage in liver and cleared from the biological system via phagocytosis as revealed by ICP-OES, VSM and Prussian blue staining results. Haematology, serum biochemistry and histology results revealed that the administered MFNPs did not induce any significant toxicity in experimental animals. Finally, biodistribution and clearance studies performed for up to 28 days demonstrated that MFNPs showed no toxicity and biocompatible, thus indicating their overall safety, and suitability for its future applications in cancer therapy, drug delivery and bioimaging.

**Acknowledgements**

The author gratefully acknowledges Indian Council of Medical Research (ICMR-SRF) and Council of Scientific and Industrial Research (CSIR), Network project-ADD (CSC0302) under XII Plan for financial assistance. The authors sincerely thank Dr. M. Kannagavel (Isebel Hospital, Chennai) for his interpretation of results in blood biochemistry and histopathology.

## References


1. J.E. Rosen, L. Chan, D.B. Shieh, F.X. Gu, Nanomedicine, 2012, **8**, 275−290.
2. S. Prijic, Sersa G, Magnetic nanoparticles as targeted delivery systems in oncology, Radiol. Oncol., 2011, **45**, 1−16.
3. W.S. Vedakumari, P. Prabu, S.C. Babu, T.P. Sastry, BBA-Gen Subjects, 2013, **1830**, 4244−4253.
4. S. Hirn, M. Semmler-Behnke, C. Schleh, A. Wenk, J. Lipka, M. Schäffler, S. Takenaka, W. Möller, G. Schmid, U. Simon, W.G. Kreyling, Eur. J. Pharm. Biopharm., 2011, **77**, 407−416.
5. A. Ruiz, Y. Hernández, C. Cabal, E. González, S. Veintemillas-Verdaguer, E. Martínez, M.P. Morales, Nanoscale, 2013, **5**, 11400−11408.
6. P. Prabu, W.S. Vedakumari, B. Santhosh Kumar, B. Sreedhar, T.P. Sastry, Mater. Chem. Phys. 2014, **148**, 1212–1220.
7. Y.M. Huh, H.T. Song, S. Kim, J.S. Choi, J.H. Lee, S. Yoon, K.S. Kim, J.S. Shin, J.S. Suh, J. Cheon, JACS, 2005, **127**, 12387–12391.
8. T. Morais, M.E. Soares, J.A. Duarte, L. Soares, S. Maia, P. Gomes, E. Pereira, S. Fraga, H. Carmo, L. Bastos Mde, Eur. J. Pharm. Biopharm., 2012, **80**, 185–193.
9. W.K. Tseng, J.J. Chieh, Y.F. Yang, C.K. Chiang, Y.L. Chen, S.Y. Yang, H.E. Horng, H.C. Yang and C.C. Wu, PLoS One, 2012, **7**, e48510.
10. L. Gu, R.H. Fang, M.J. Sailor, J.-H. Park, ACS Nano, 2012, **6**, 4947–4954.
11. M. Levy, N. Luciani, D. Alloyeau, D. Elgrabli, V. Deveaux, C. Pechoux, S. Chat, G. Wang, N. Vats, F. Gendron, C. Factor, S. Lotersztajn, A. Luciani, C. Wilhelm and F. Gazeau, Biomaterials, 2011, **32**, 3988–3999.
12. C. R. Valois, J. M. Braz, E. S. Nunes, M. A. Vinolo, E. C. Lima, R. Curi, W. M. Kuebler and R. B. Azevedo, Biomaterials, 2010, **31**, 366–374.

13. A.J. Cole, A.E. David, J. Wang, C.J. Galbán, V.C. Yang, Biomaterials, 2011, **32**, 6291–6301.

14. Z. Cheng, Y. Dai, X. Kang, C. Li, S. Huang, H. Lian, Z. Hou, P. Ma, J. Lin, Biomaterials, 2014, **35**, 6359–6368.

15. M.J. Lee, O. Veiseh, N. Bhattarai, C. Sun, S.J. Hansen, S. Ditzler, S. Knoblaugh, D. Lee, R. Ellenbogen, M. Zhang, J.M. Olson, PLoS One, 2010, **5**, e9536.

16. P. Prabu, W.S. Vedakumari, B. Santhosh Kumar, B. Sreedhar, T.P. Sastry, Mater. Lett., 2014, **139**, 108−111.

17. O. Hiraku, M. Yoshiharu, Biomaterials, 1999, **20**, 175–182.

18. T.K. Jain, M.K. Reddy, M.A. Morales, D.L. Leslie-Pelecky, V. Labhasetwar, Mol. Pharm., 2008, **5**, 316–327.

19. R.P. Beliles, A.K. Palmer, Toxicology, 1975, **5**, 147–158.

20. P. Storey, R.P. Lim, H. Chandarana, A.B. Rosenkrantz, D. Kim, D.R. Stoffel, V.S. Lee. Invest. Radiol. 2012, **47**, 717–724.

21. G. Shahnaz, C. Kremser, A. Reinisch, A. Vetter, F. Laffleur, D. Rahmat, J. Iqbal, S. Dünnhaupt, W. Salvenmoser, R. Tessadri, U. Griesser, A. Bernkop-Schnürch. Eur. J. Pharm. Biopharm., 2013, **85**, 346–355.

22. X.D. Zhang, D. Wu, X. Shen, P.X. Liu, N. Yang, B. Zhao, H. Zhang, Y.M. Sun, L.A. Zhang and F.Y. Fan, Int. j. Nanomedicine 2011, **6**, 2071–2081.

23. K.R. Di Bona, Y. Xu, P.A. Ramirez, J. DeLaine, C. Parker, Y. Bao, J.F. Rasco JF. Reprod Toxicol. 2014, **50**, 36-42.

24. L. Yang, H. Kuang, W. Zhang , Z.P. Aguilar, Y. Xiong, W. Lai, H. Xu, H. Wei. Nanoscale. 2015, **7**, 625-636.

25. P. Venkatesan, N. Puvvada, R. Dash, B.N. Prashanth Kumar, D. Sarkar, B. Azab, A. Pathak, S.C. Kundu, P.B. Fisher, M. Mandal. Biomaterials. 2011, **32**, 3794-3806.

26. W.S. Vedakumari, P.Prabu, T.P.Sastry. J. Biomed. Nanotechnol. 2015, **11**, 657-667.

27. C. He, Y. Hu, L. Yin, C. Tang, C. Yin, Biomaterials, 2010, **31**, 3657–3666.

28. B. Semete, L. Booysen, Y. Lemmer, L. Kalombo, L. Katata, J. Verschoor, H.S. Swai, Nanomedicine, 2010, **6**, 662–671.

29. M. Longmire, P.L. Choyke, H. Kobayashi. Nanomedicine, 2008, **3**, 703-717.

30. Wahajuddin, S. Arora. Int J Nanomedicine. 2012; **7**, 3445–3471.

31. H.S. Choi, W. Liu, P. Misra, E. Tanaka, J.P. Zimmer, B. Itty Ipe, M.G. Bawendi, J.V. Frangioni. Nature Biotechnology, 2007, **25**, 1165 – 1170.

32. K. Briley-Saebo, A. Bjørnerud, D. Grant, H. Ahlstrom, T. Berg, G.M. Kindberg, Cell Tissue Res., 2004, **316,** 315–323.

33. R.S. McCuskey, P.A. McCuskey, R. Urbaschek, B, Urbaschek. Infect. Immun. 1984, **45**, 278–280.

34. Y. Yang, Y. Sun, Y. Liu, J. Peng, Y. Wu, Y. Zhang, W. Feng, F. Li. Biomaterials, 2013, **34**, 508–515.

35. B. Zhang, Q. Li, P. Yin, Y. Rui, Y. Qiu, Y. Wang, D. Shi. ACS Appl Mater Interfaces. 2012, **4**, 6479-6486.

36. R. Weissleder, D.D. Stark, B.L. Engelstad, B.R. Bacon, C.C. Compton, D.L. White, P. Jacobs, J. Lewis, Am. J. Roentgenol., 1989, **152**, 167–173.

37. D. Pouliquen, J.J. Le Jeune, R. Perdrisot, A. Ermias, P. Jallet, Magnetic Resonance Imaging, 1991, **9**, 275–283.

38. X.D. Zhang, D. Wu, X. Shen, P.X. Liu, F.Y. Fan, S.J. Fan, Biomaterials, 2012, **33,** 4628–4638.

39. S. Song, B. Xia, J. Chen, J. Yang, X. Shen, S. Fan, M. Guo, Y. Sun, RSC Advances 2014, **4**, 42598–42603.

40. K. Yang, J. Wan, S. Zhang, Y. Zhang, S. Lee, Z. Liu, ACS Nano., 2011, **5,** 516–522.

41. X. Huang, L. Li, T. Liu, N. Hao, H. Liu, D. Chen, F. Tang, ACS Nano., 2011, **5**, 5390–5399.

42. Y. Tang, S. Han, H. Liu, X. Chen, L. Huang, X. Li, J. Zhang, Biomaterials, 2013, **34**, 8741−8755.

**Figure caption**

Fig. 1 a) TEM image of spherical shaped MFNPs. Dynamic light scattering data showing the hydrodynamic size (in Diameter) and surface charge of MFNPs in PBS (b & c). d) Representative microscope images for Prussian blue stained Saos2 cells after incubation with MFNPs at 37 ° C for 5 h; Iron oxide nanoparticles appear blue and cells appear red in colour. e) Digital images of eppendorf-tubes containing supernatant from RBCs exposed to different concentrations of MFNPs. PBS, and water were used as negative and positive controls, respectively; Graphical representation of percentage of hemolysis by different iron concentration of MFNPs.

Fig. 2 a) Fluorescence emission spectra of FITC and FITC@MFNPs. b) Photographic images of FITC@MFNPs under normal light and UV light. c) Blood circulation curves and half-time of FITC@MFNPs in blood after intravenous injection in experimental animals.

Fig. 3 a) Biodistribution profile of MFNPs in the organs excised after intravenous administration in mice. b) Distribution of MFNPs in liver at 6, 12, and 24 h. Table. 1) Clearance of nanoparticles in animal urine and faecal samples at various time intervals.

Fig. 4 Prussian blue staining. The various organs of control and experimental animals excised after 1, 7, 14 and 28 d of MFNPs injection and stained with Prussian blue. The stained liver, spleen, lung, heart and kidney sections were visualized at 40 X

under bright field microscope. The insets in liver section indicate the magnified image of kupffer cells.

Fig. 5 a) Body weight measurement in control and experimental animals after every 2 days of MFNPsinjection for 28 days. b) Analysis of spleen and thymus indexes in control and experimental animals after 1 d and 28 d of MFNPs injection.

Fig. 6 Hematology and serum biochemical analysis. Time-course measurement of levels of WBC, RBC, PLT, HGB, HCT, AST, ALT, CREA and BUN in the control and experimental animals after 1, 7, 14 and 28 d of MFNPs injection. The asterisk symbol (*) represents the statistically significant difference from control ($P<0.05$) as determined by the Student t test.

Fig. 7 Haematoxylin and Eosin (H & E) staining. Representative photomicrographs of liver, spleen, lung, heart and kidney tissues from control and experimental animals after 1, 7, 14 and 28 days of MFNPs injection. Magnification – 40 X.

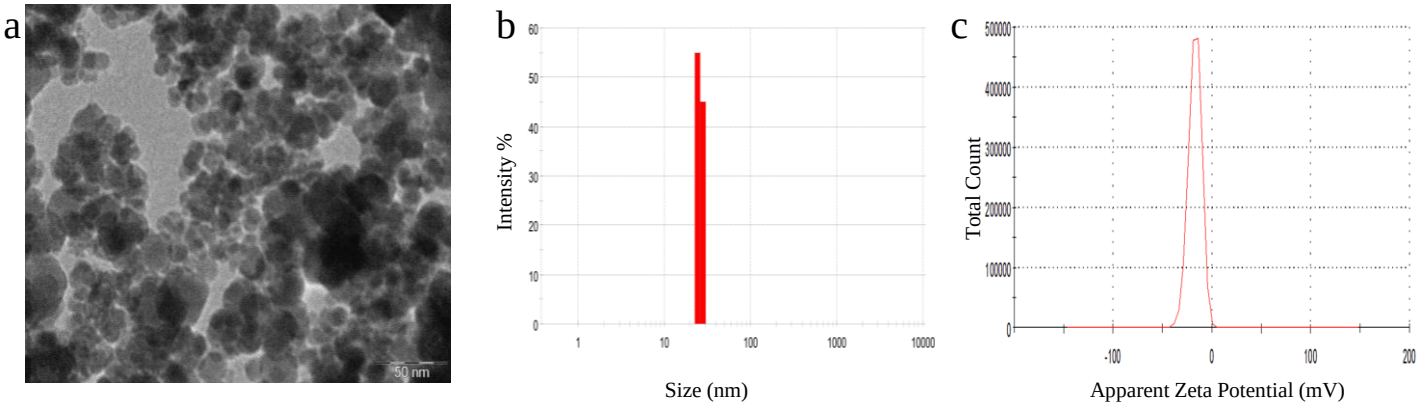


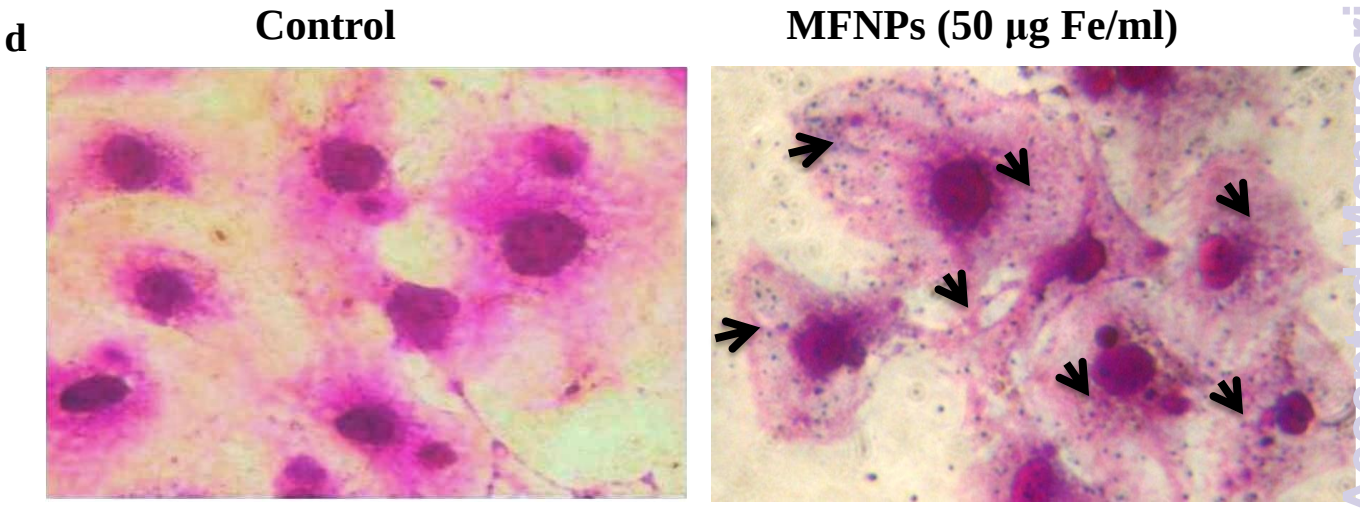


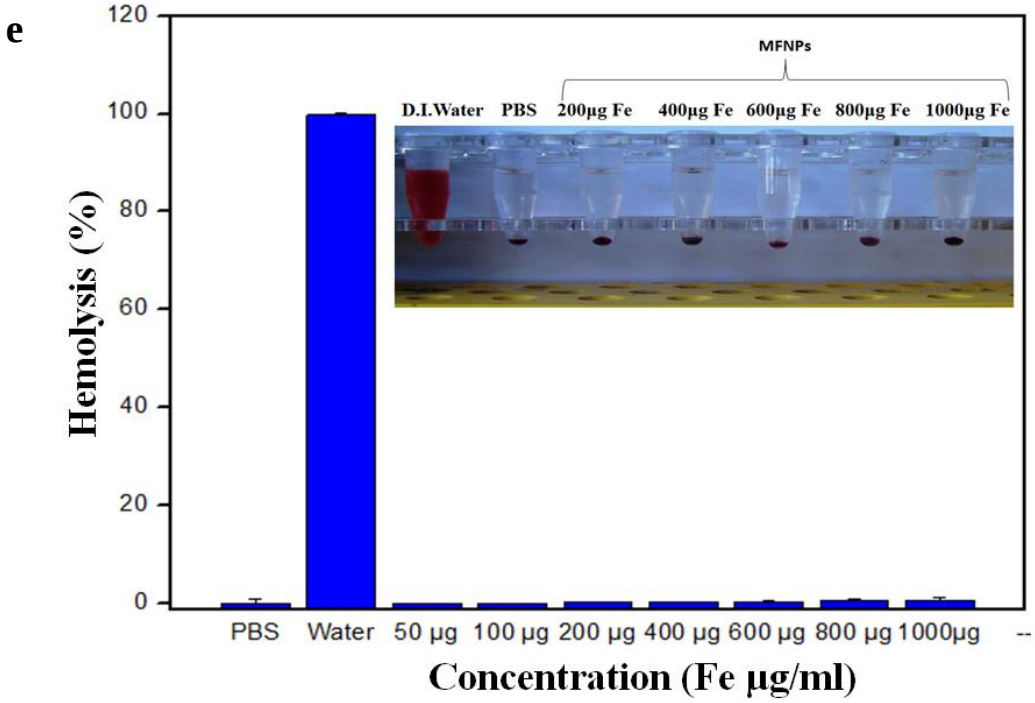

# Fig. 2.

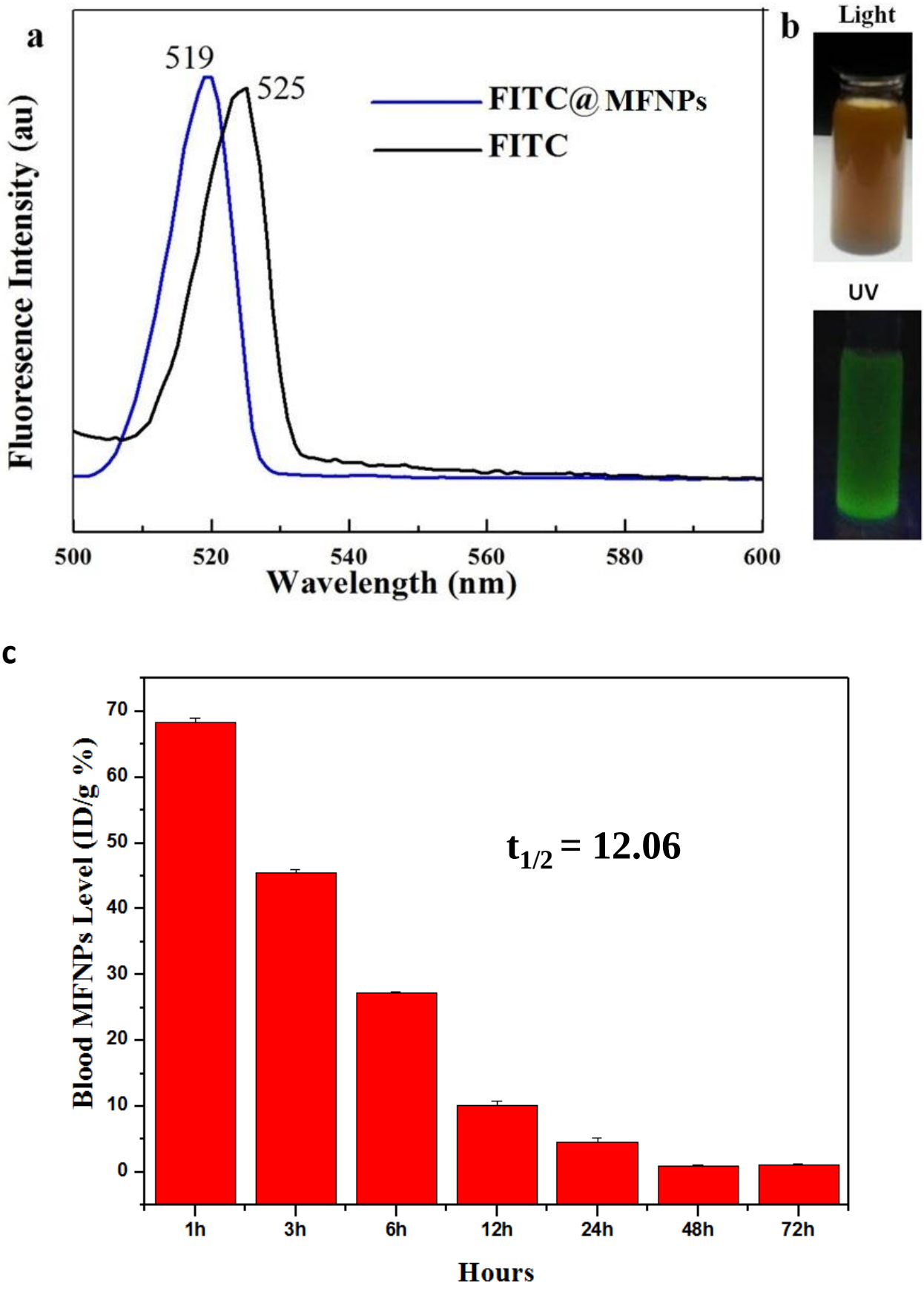

# Fig. 3

a

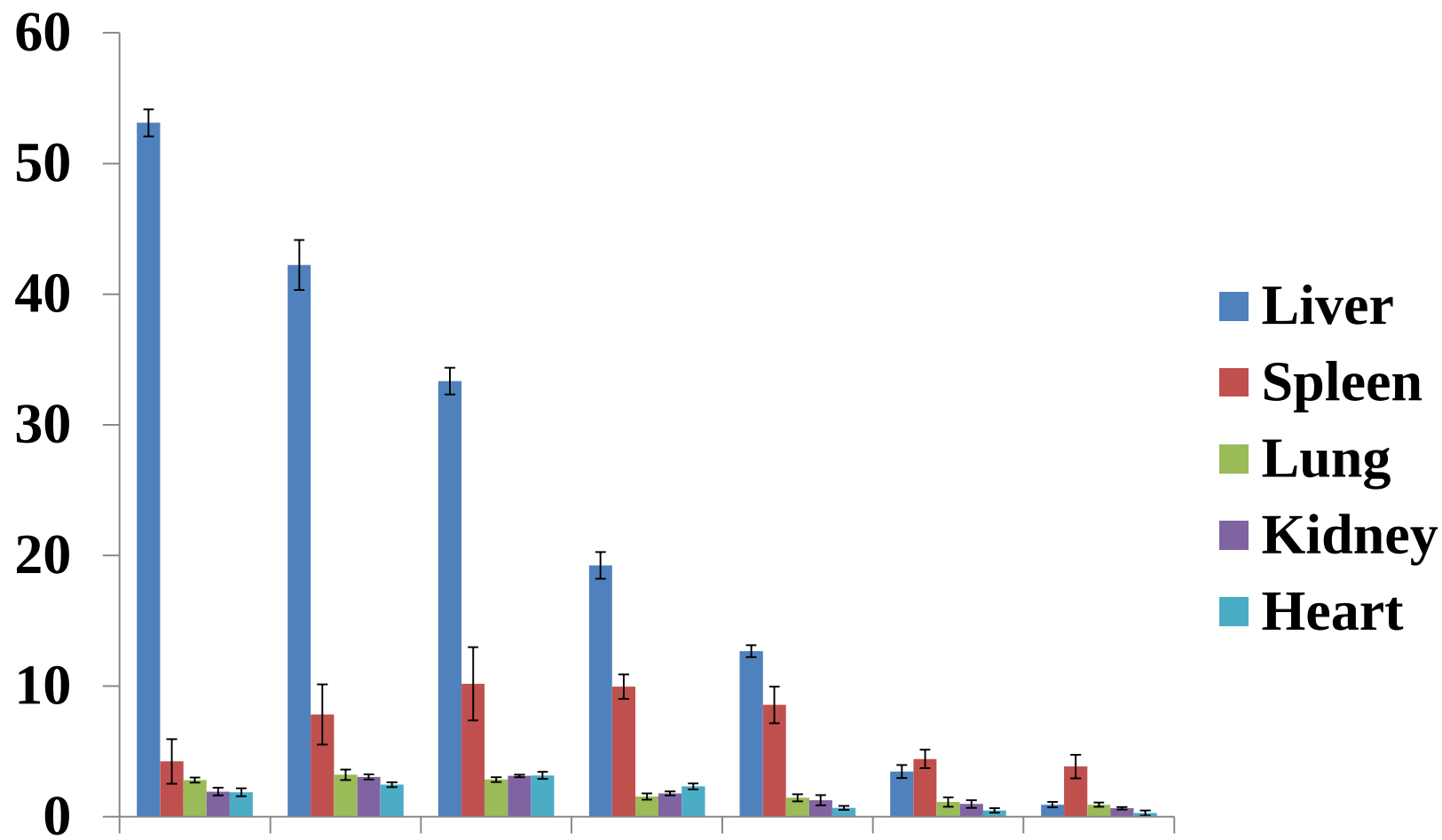


b

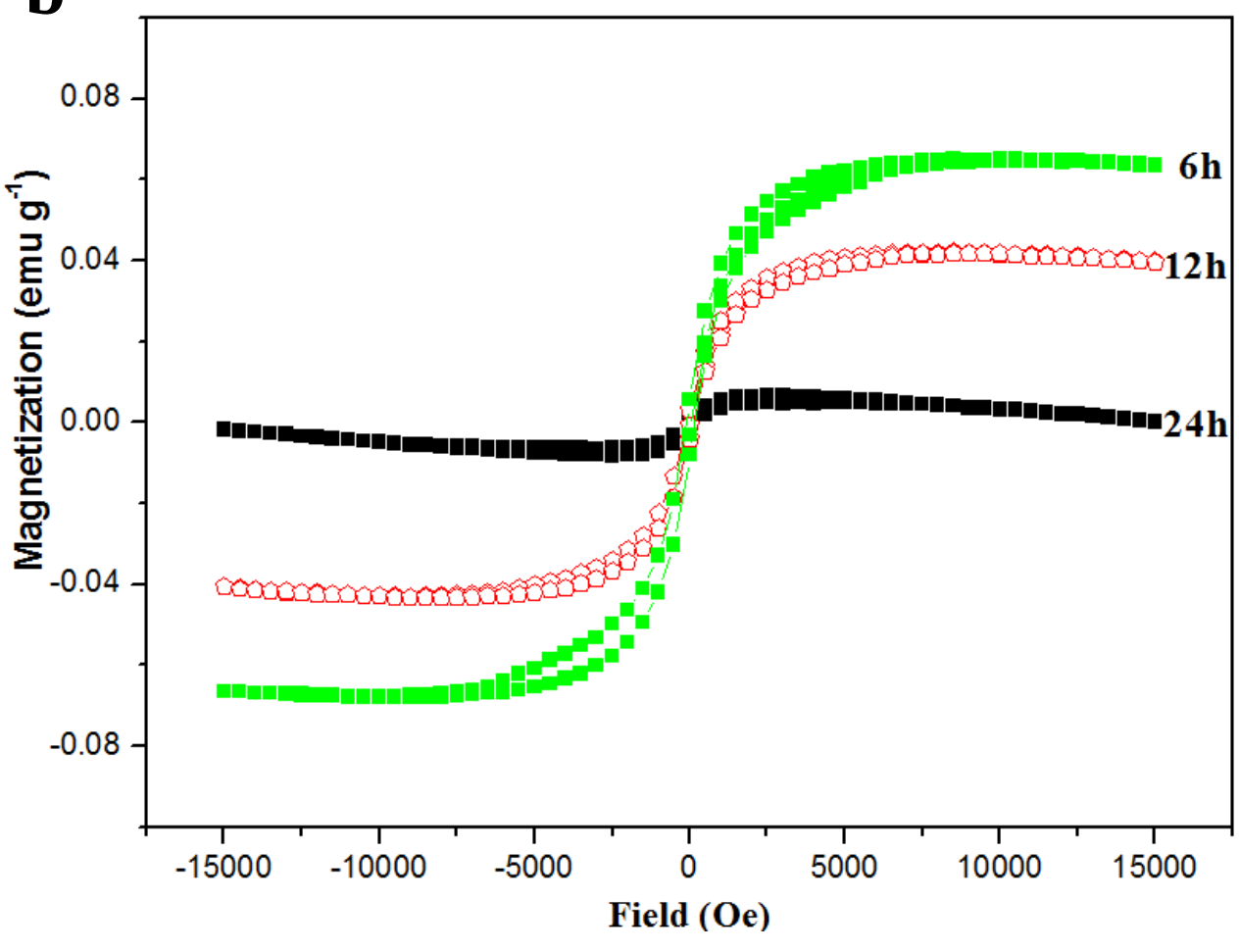


c

| Time | Urine (ID/g %) | Feces (ID/g %) |
|---|---|---|
| 6 h | 0.67±0.34 | 1.32±0.19 |
| 12 h | 1.72±0.42 | 1.56±0.34 |
| 24 h | 1.08±0.33 | 1.33±0.70 |
| 3d | 1.04±0.78 | 1.12±0.43 |
| 7d | 0.81±0.23 | 1.02±0.34 |

# Fig. 4.

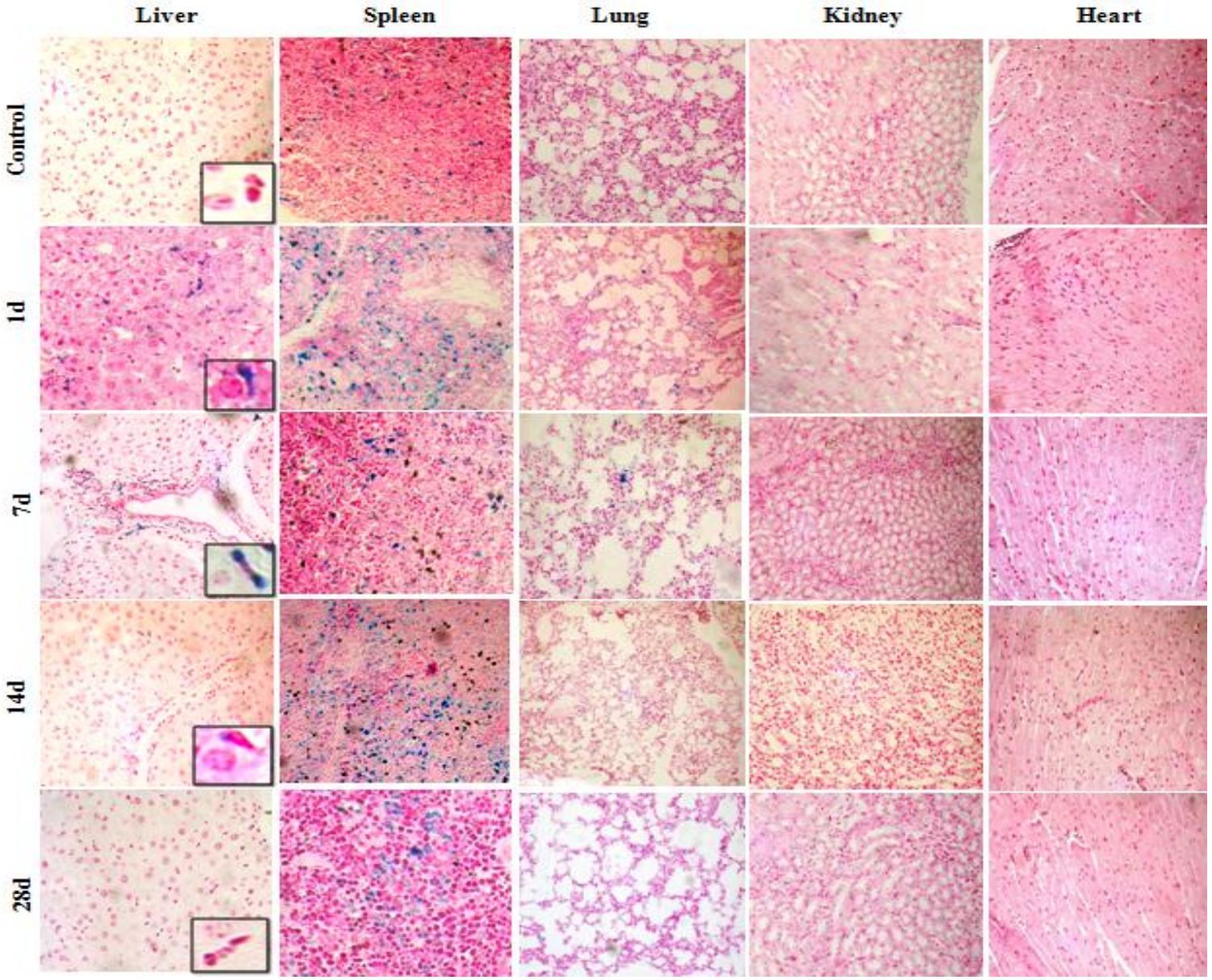

# Fig. 5

**a**

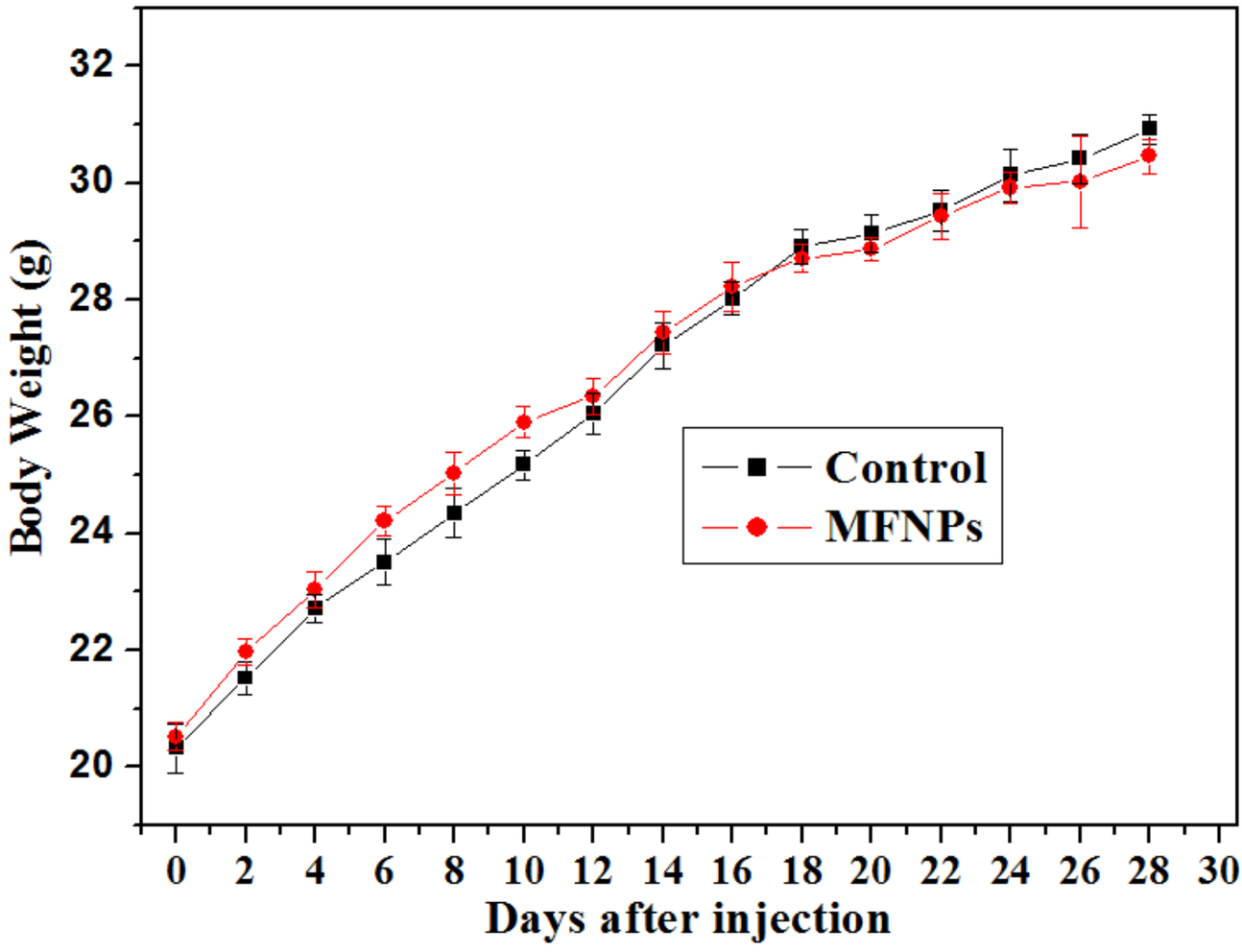


**b**

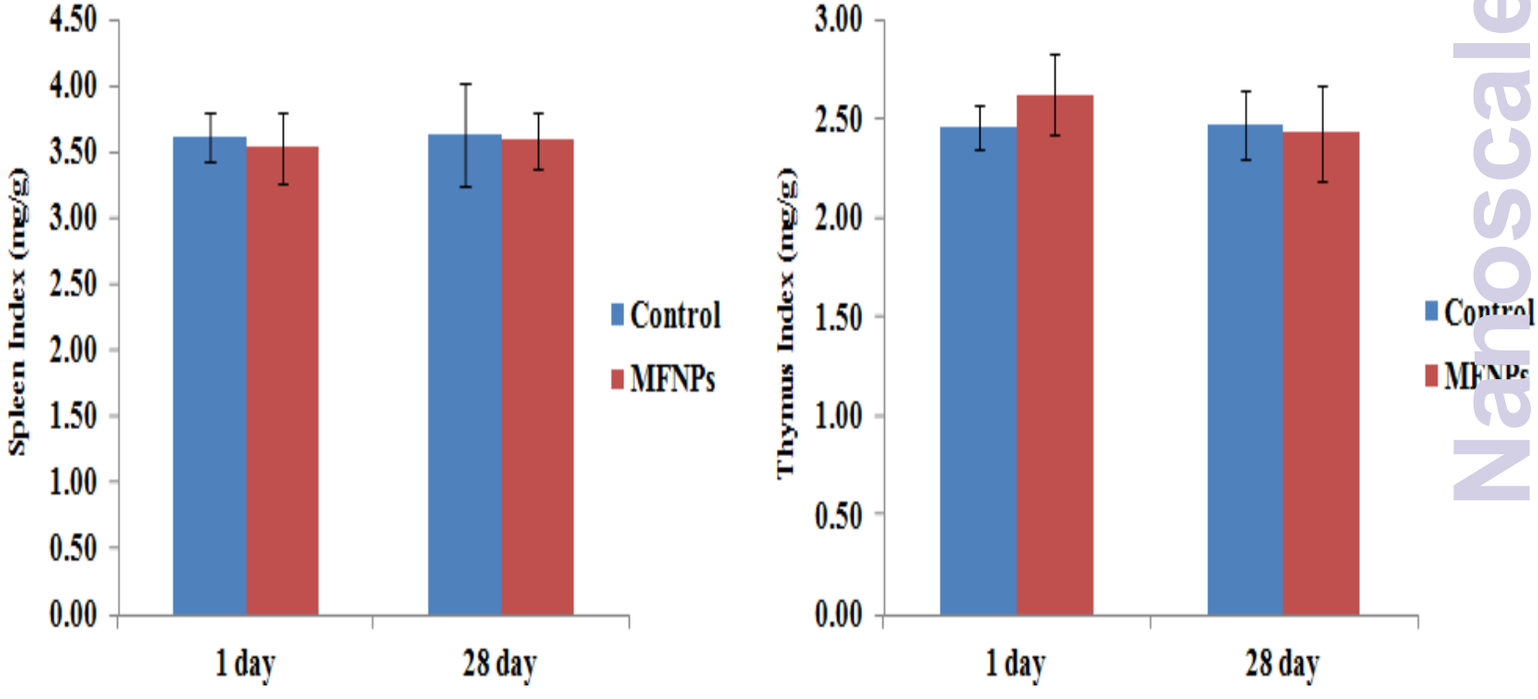

# Fig. 6

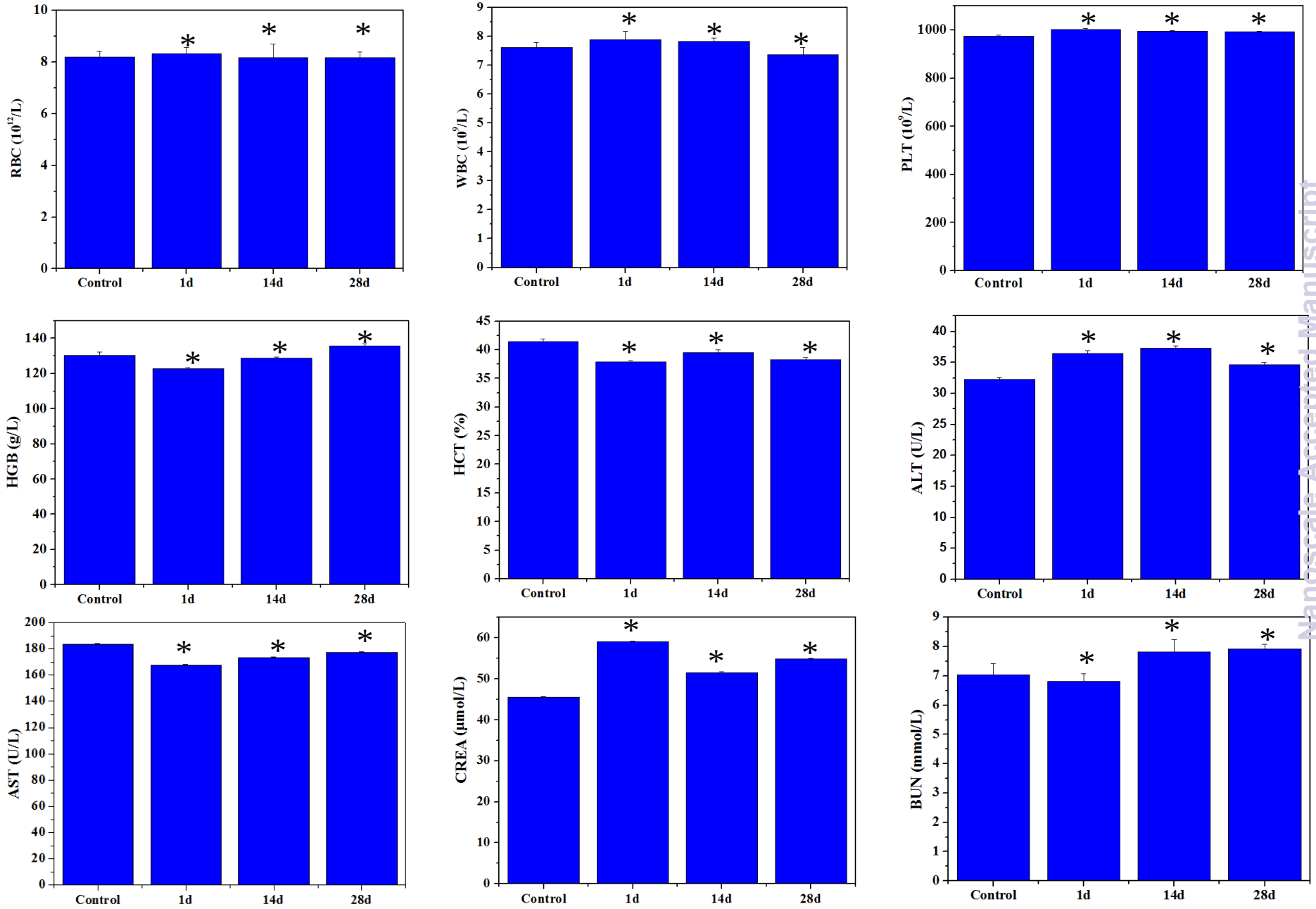

# Fig. 7.